Computer Science and Information Technologies
Vol. 6, No. 2, July 2025, pp. 169~177
ISSN: 2722-3221, DOI: 10.11591/csit.v6i2.p169-177

HepatoScan: Ensemble classification learning models for liver cancer disease detection

Tella Sumallika[1], Raavi Satya Prasad[2]
[1]Department of Computer Science and Engineering, Acharya Nagarjuna University, Guntur, India
[2]Department of Computer Science and Engineering, Dhanekula Institute of Engineering and Technology, Vijayawada, India

Article Info

Article history:

Received Oct 26, 2024
Revised Jan 23, 2025
Accepted Feb 20, 2025

Keywords:

Angiosarcoma
Cholangiocarcinoma
Deep learning
Ensemble classification
Hepatocellular carcinoma
HepatoScan

ABSTRACT

Liver cancer is a dangerous disease that poses significant risks to human health. The complexity of early detection of liver cancer increases due to the unpredictable growth of cancer cells. This paper introduces HepatoScan, an ensemble classification to detect and diagnose liver cancer tumors from liver cancer datasets. The proposed HepatoScan is the integrated approach that classifies the three types of liver cancers: hepatocellular carcinoma, cholangiocarcinoma, and angiosarcoma. In the initial stage, liver cancer starts in the liver, while the second stage spreads from the liver to other parts of the body. Deep learning is an emerging domain that develops advanced learning models to detect and diagnose liver cancers in the early stages. We train the pre-trained model InceptionV3 on liver cancer datasets to identify advanced patterns associated with cancer tumors or cells. For accurate segmentation and classification of liver lesions in computed tomography (CT) scans, the ensemble multi-class classification (EMCC) combines U-Net and mask region-based convolutional network (R-CNN). In this context, researchers use the CT scan images from Kaggle to analyze the liver cancer tumors for experimental analysis. Finally, quantitative results show that the proposed approach obtained an improved disease detection rate with mean squared error (MSE)-11.34 and peak signal-to-noise ratio (PSNR)-10.34, which is high compared with existing models such as fuzzy C-means (FCM) and kernel fuzzy C-means (KFCM). The classification results obtained based on detection rate with accuracy-0.97%, specificity-0.99%, recall-0.99%, and F1S-0.97% are very high compared with other existing models.

This is an open access article under the CC BY-SA license.

Corresponding Author:

Tella Sumallika
Department of Computer Science and Engineering, Acharya Nagarjuna University
Nagarjuna Nagar-522510, Andhra Pradesh, India
Email: sumallika.p@gmail.com

1. INTRODUCTION

The liver is a typical organ in the human body that regulates chemical levels in the blood and excretes a substance called bile. The primary purpose of bile is to transport waste material from the liver. Liver cancer is a significant contributor to global malignancy mortality, making up a significant portion of all malignant death categories [1]. Because liver cancer, particularly hepatocellular carcinoma, has demonstrated promising treatment efficacy and improved survival when diagnosed at an earlier stage, elucidating molecular biomarkers or mechanisms for early detection is crucial [2], [3]. We also validate the measurements against other clinical standards, such as biopsy, which remains the gold standard for detection,

and traditional imaging techniques like ultrasound. However, both of these methods have limitations, including low accuracy, time-consuming nature, potential expense, and the possibility of human error [4].

Advances in medical image processing and deep learning algorithms represent a promising prospect for overhauling cancer detection as we currently know it [5]. These methods could help radiologists and oncologists to better detect cancerous tissues by automating the analysis of medical images. Image processing is crucial in upgrading the quality and beautifying medical images for diagnosis [6]. Meanwhile, deep learning algorithms, particularly convolutional neural networks (CNNs), perform best for detecting and classifying liver cancer pathology on medical images [7]. This includes using various identified image modalities like computed tomography (CT), magnetic resonance imaging (MRI), and ultrasound scans. We process these images using several techniques to extract the required features, and then employ deep learning models to determine whether abnormal growth is present in healthy tissues [8]. By identifying patterns in large datasets of labeled images, deep learning models can aid in early diagnosis, tumor segmentation, and cancer progression prediction. However, despite these setbacks, applying image processing and deep learning algorithms in liver cancer detection is highly promising [9], [10].

In this research work, the proposed approach is the combination of U-Net and Mask region-based convolutional network (R-CNN). U-Net concentrated on segmentation, while Mask R-CNN handled classification. We use InceptionV3 to train images of liver cancer and normal CT scans. We utilize transfer learning to transfer the frozen layers to the proposed ensemble multi-class classification (EMCC), which enhances lesion detection. Finally, the proposed EMCC shows the performance in terms of detecting the cancer-affected regions and classification of images. Figure 1 shows the methods used in this work.

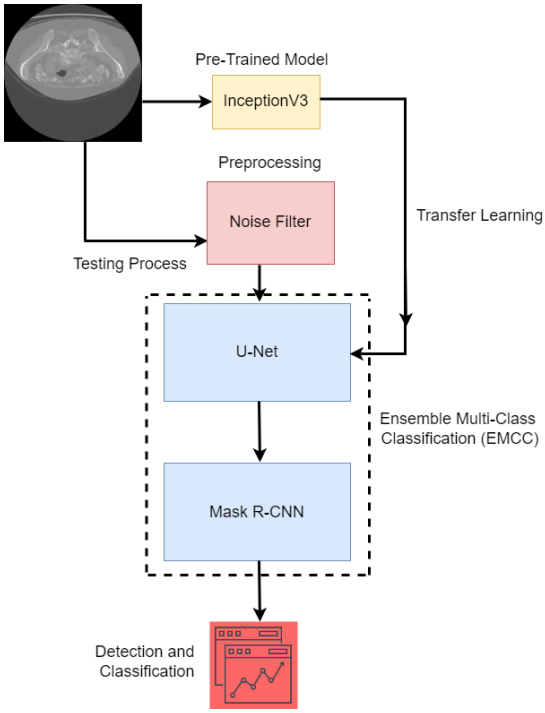

Figure 1. The architecture of EMCC

2. LITERATURE SURVEY

Zhen *et al.* [11] introduced a new deep learning system (DLS) that diagnoses and detects liver tumors in the early stages using MRI scan images. The proposed approach mainly focused on classifying liver tumors into seven types. The results show that the proposed approach obtained a high accuracy of 92.34% based on the detection rate. There is the lack of accuracy based on the disease detection. Alirr [12] proposed an advanced learning approach that segments the liver samples from the CT scan images. It is the combination of FCN and region-based level techniques. The proposed approach segments the liver organ from the input CT scan image to find the tumors. In the final step, the region-based level refined the segmentation prediction to identify the accurate final segmentation. The results demonstrate that the proposed approach produces accurate results. There is lack of segmentation results in this approach. Sumallika and Prasad [13] presented a

combined model for detecting liver cancer and diseases in their early stages. In this application, the ResNet50 is a pre-trained model that extracts features and filters out noise from input images. The proposed method combines extreme gradient boosting (EGB) and recurrent neural network (RNN) to detect unusual cancer cells and achieves a higher accuracy of 98.48%.

Rela *et al*. [14] introduced a new optimization algorithm that adopts the U-Net features that combine with grey wolf-class topper optimization (GW-CTO). The features are extracted using the training model that selects the features belonging to hyper-parameter tuned improved-deep neural network (HI-DNN) enhanced by the same GW-CTO algorithm. In the final step, the GW-CTO-HI-DNN improved the accuracy up to 4.3%, 2.4%, 5.2%, and 4.3% for all the other models. The proposed approach has high accuracy compared with other models. Liu *et al*. [15] introduced AI-based models that detect liver tumors using advanced segmentation combined with a K-means clustering (KMC) algorithm. The proposed model diagnoses the liver tumors and classifies the normal and tumor CT images. The experiments show that the liver tumor obtains an accuracy of 93.23%. Di *et al*. [16] demonstrated an automated approach for segmenting liver CT scan images and extracting liver tumours. In this case, the segmentation difficulties are mitigated by using the 3D U-Net to divide the high-resolution pixels using local information based simple linear iterative clustering (LI-SLIC)-based hierarchical iterative segmentation. Finally, the voting model is utilised to extract tumour regions from high-resolution pixels, identify abnormal areas, and classify pixel-based results. The results demonstrate that the proposed approach produces accurate results.

Li *et al*. [17] proposed a deep attention-based neural network with high-resolution and multi-scale characteristics for liver and tumour segmentation in CT scan pictures. The multi-scale features alter the fusion, allowing fields to modify the liver and tumour to various forms and sizes. Finally, the proposed strategy improves performance. Gunasekhar *et al*. [18] proposed a new deep learning -based model combined with an optimization algorithm. This work combines six filters with feature selection to improve the final outcomes. Among these filters, two high-dimensional features are extracted using the modified social ski-driver optimization (MSSO) algorithm. These extracted features, also called high-ranked features, find the accurate features from the liver cancer tissues detected by the sunflower optimization-based deep neural network (DSFNN) approach. The experimental analysis was applied to the National Center for Biotechnology Information-Gene Expression Omnibus (NCBI-GEO) database, and superior performance was obtained in classifying types of liver cancers. Baâzaoui *et al*. [19] stated a semi-automated segmentation method for numerous lesions in the liver using CT scan data. The recommended approach removes liver lesions from the input images and classifies them as normal or abnormal images. The results suggest that the proposed strategy outperforms other models in terms of classification accuracy. Das *et al*. [20] proposed the model kernel fuzzy C-means (KFCM) clustering combined with adaptive and morphological processing models that segment the liver CT scan morphological images. KFCM is also used to reduce the noise and increase the strength of the clustering. The quantitative results show that the proposed approach obtains better peak signal-to-noise ratio (PSNR) and low mean squared error (MSE) with consistent accuracy.

3. DATASET DESCRIPTION

Liver tumour segmentation challenge 2017 (LiTS17) dataset is the most often used [21]. It contains CT scan images of liver tumours from a variety of people. Each sample has 3D scan segmentation markings representing liver areas and liver tumours. It comprises 500 CT scan liver photos, including 300 training and 200 CT scan images. Figure 2 shows the CT scan images from the dataset.

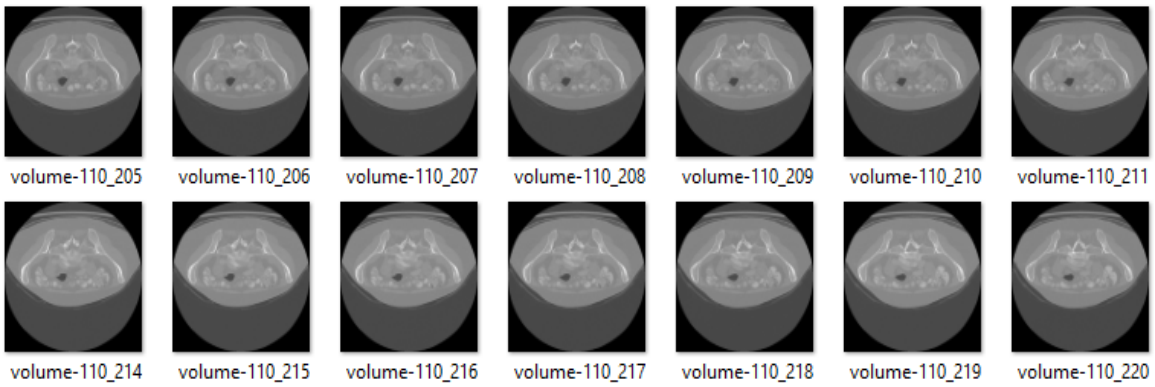

Figure 2. Sample liver CT images from dataset

4. PRE-TRAINED MODEL INCEPTIONV3

The architecture of InceptionV3 is populated with several manifold modules from the third-order moment sequence pool, which are conceptually suitable for learning coarse and mid-level abstractions. Analysis of liver tumors often involves distinguishing between low-contrast subtle textures and patterns that could characterize cancerous cells. Hence, high-resolution feature extraction is essential. Further fine-tuning InceptionV3 on liver tumor data from our institution enables the model to tweak its learned features and recognize any liver-specific anomalies or differences in their morphology, hence allowing better detection performance [22]. The pre-trained layers in InceptionV3 have already learned to detect the best complex textures and patterns in images, training (fine-tuning) the model on medical imaging datasets with slight adaptation. It mainly allows the deep and diverse convolutional structures to capture the significant features crucial for differentiating liver tumors and non-tumor tissues [23]. This model mainly reduces the computational demands and improves pattern detection with rapid outcomes.

The structure of InceptionV3 mainly consists of rich feature extraction layers. The model loaded the weights for liver cancer detection but ignored the top layer, which allows customization to classify normal and abnormal samples. The classification improved by adding the dense and dropout layers to the default InceptionV3, which involves the fully connected layer using softmax activation for multi-class classification, represented in (1).

$$\text{InceptionV3}_{\text{model}} = \text{InceptionV3}\left(\text{weights} = \text{'imagenet'},\ \text{include}_{\text{top}} = \text{False},\ \text{input}_{\text{shape}} = (299, 299, 3)\right) \quad (1)$$

Transfer learning is mainly used to fine-tune the top layers of InceptionV3, which initially keeps the lower layers frozen to retrieve the pre-trained features. The total number of trainable layers $L_{\text{trainable}}$ is represented in (2):

$$\theta = \{w_i \epsilon\ L_{\text{trainable}} \mid \text{Freeze}\ L_{\text{frozen}}\} \quad (2)$$

Loss function (L): the binary cross-entropy used for binary classification for multiclass is represented in (3):

$$L = -\frac{1}{N}\sum_{i=1}^{N} y_i \cdot \log(\hat{y}_i) \quad (3)$$

Optimizer: the Adam optimizer used to improve the learning rate of for 10^{-4} fine tuned layers represented in (4):

$$\theta \leftarrow \theta - \alpha \cdot \nabla_\theta L(\theta) \quad (4)$$

Where, α is learning rate and L is loss function.

5. ENSEMBLE MULTI-CLASS CLASSIFICATION

Combining U-Net and Mask R-CNN for liver cancer detection is a successful merger because they have strengths that make them particularly well-suited to medical imaging tasks. U-Net, famous for its performance in semantic segmentation problems, dominates pixel-level classification by taking advantage of image resolutions at different scales. The proposed network uses a symmetric encoder-decoder U-Net architecture with skip connections, allowing for great localization and making it well-suited to segmenting tumors or other abnormalities in high-complexity anatomical structures like the liver. In contrast, Mask R-CNN extends Faster R-CNN by adding instance segmentation (localized pixel-wise image categorization) to the top of object detection. This makes it possible to perform tumor localization and liver tumor delineation in a single slice coordinate map paired with the input CT scan. It will use a two-stage detection algorithm, where the regions are initially proposed. Then, these regions are refined while simultaneously creating object masks, bounding boxes, and classifying labels. This multi-task processing is beneficial in separating and segmenting individual tumors in the case of multiple liver lesions. U-Net is typically used as a preparatory and initial liver area segmentation of the framework within an integrated model for detecting liver cancer. It is beneficial to Mask R-CNN by ensuring it can target liver tumors more directly and accurately instead of a more significant portion. Alternatively, the segmentation map of U-Net can guide Mask R-CNN's region proposals on tumor boundaries and consequently increase localization accuracy around instance masks. Finally, the combined model improves the detection rate in terms of accuracy, quality of segmentation, and understanding, which introduces a more robust model for diagnosing liver cancer.

Step 1: Input image processing and preprocessing
Image normalization: the input image I is normalized by deducting the intensity of the mean and dividing by the standard deviation σ given in (5).

$$I_{norm} = \frac{1-\mu}{\sigma} \quad (5)$$

Resizing: the input image is resized to a fixed size that is compatible with the network, such as H X W.
Step 2: Initial segmentation with U-Net
The U-Net functionality is mainly used to segment the liver region by isolating the region of interest (ROI) that is most likely to contain the liver.

a) Downsampling path (encoder):
   – The spatial dimensions are reduced by using the convolutional layers to capture the feature representations.
   – The filter f is applied at every convolution layer, and X as input, followed by ReLU activation:

$$X_{conv} = \text{ReLU}(f * X + b) \quad (6)$$

   – To downsample the feature maps, max-pooing is applied after convolution:

$$X_{pool} = \text{MaxPool}(X_{conv}) \quad (7)$$

b) Bottleneck layer: this layer captures the core features by combining the high-level semantics from the encoder with accurate upsampling details.
c) Upsampling path (decoder):
   – Transmit the convolutions upsample the feature maps:

$$X_{upsample} = \text{TransposeConv}(X_{pool}) \quad (8)$$

   – The skip connections are integrated with the upsampled features to retrieve the spatial data.
d) Output segmentation mask (liver ROI):
   – The U-Net outputs a binary mask, M_{Liver} where:

$$M_{liver}(x,y) = \begin{cases} 1 & \text{if}(x,y) \in \text{liver region} \\ 0 & \text{otherwise} \end{cases} \quad (9)$$

Step 3: Filtered instance segmentation with Mask R-CNN
In this step, the U-Net performed the typical segmentation to find any cancerous regions (cells) in the liver.

a) Region proposal network:
   – For every input image, the bounding box is used to set the region proposals.
   – For every anchor box, p represents the objectness score, which is measured as:

$$p = \sigma(w \cdot f(X) + b) \quad (10)$$

   – All the boxes with high objectness scores initialize strong cancer lesions.
b) Mask prediction: for every ROI, a binary mask M_{Lesion} is constructed for the lesion occurrences.

$$M_{Lesion}(x,y) = \begin{cases} 1 & \text{if}(x,y) \in \text{Lesion region} \\ 0 & \text{otherwise} \end{cases} \quad (11)$$

c) Filtering bounding box and prediction of class:
   – In this context, the network filters the bounding box coordinates $B = (x, y, w, h)$ and initializes class labels based on the probability of lesion existence.

Step 4: Final layer - integrated mask and bounding box
The final layer contains:
   – From U-Net, the liver mask represented as M_{Liver}.
   – The Mask R-CNN M_{Lesion} and B obtain the lesion masks and bounding boxes.

In the final step, the ensemble approach used to impove the accuracy based on the detection rate.

6. RESULTS AND DISCUSSION

In this context, the proposed algorithm EMCC is implemented using Python with better libraries such as Keras, Pandas, and Numpy. The tumor or cancer detection and classification is measured by using the confusion matrix applied to CT scan images. The combined approach, U-Net and Mask R-CNN, mainly focused on segmentation and finding accurate lesions using the bounding box. The pre-trained model InceptionV3 is used to extract the significant features that obtain the abnormalities present in the input image. The following equations are used to measure the detection and classification rate:

MSE: The MSE measures the average squared difference between the predicted and original values. In this context, the MSE measures the segmentation outcomes by predicting the tumor size. The equation of the MSE is measured as (12):

$$\text{MSE} = \frac{1}{n}\sum_{i=1}^{n}(y_i - \hat{y}_i)^2 \tag{12}$$

PSNR: This ratio is generally used to measure the quality of the actual input image and processed image, typically in decibels (dB). It is mainly focused on measuring how the actual image differentiates from noise filters and transmission.

$$\text{PSNR} = 10 \cdot \log_{10}\left(\frac{\text{MAX}^2}{\text{MSE}}\right) \tag{13}$$

The performance of existing algorithms is compared with the fuzzy C-means (FCM) and KFCM shown in Table 1. These results represent the quality of the final output. Figure 3 shows the comparative performance between MSE and PSNR. The EMCC obtained the MSE of 11.34 and PSNR with 10.34% which is high compare with existing models.

Table 1. The quantitative performance of algorithms

	FCM	KFCM [20]	EMCC
MSE	3.456	9.531	11.34
PSNR	2.675	8.541	10.34

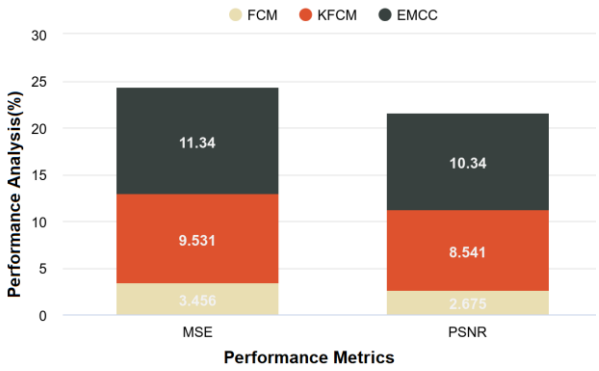

Figure 3. The performance of algorithms based on the quality of detecting the cancer regions in the input images

Among all the models the proposed ECMM shows the high-quality images after the pre-processing and feature extraction techniques. Figure 4 shows the difference between original CT scan image and cancer prediction image. The classification parameters are shown based on the strength of the proposed approach. These parameters are obtained from the confusion matrix. The classification results based on the detection rate and these are measured by using the following:

$$\text{Accuracy (ACC)} = \frac{\text{TP+TN}}{\text{TP+TN+FP+FN}} \tag{14}$$

$$\text{Specificity (Spc)} = \frac{\text{No of TN}}{\text{No of TN+ No of FP}} \tag{15}$$

$$\text{Recall (Re)} = \frac{\text{TP}}{\text{TP+ FN}} \quad (16)$$

$$\text{F1} - \text{score (F1S)} = 2 * \frac{(\text{Precision} * \text{Recall})}{(\text{Precision} + \text{Recall})} \quad (17)$$

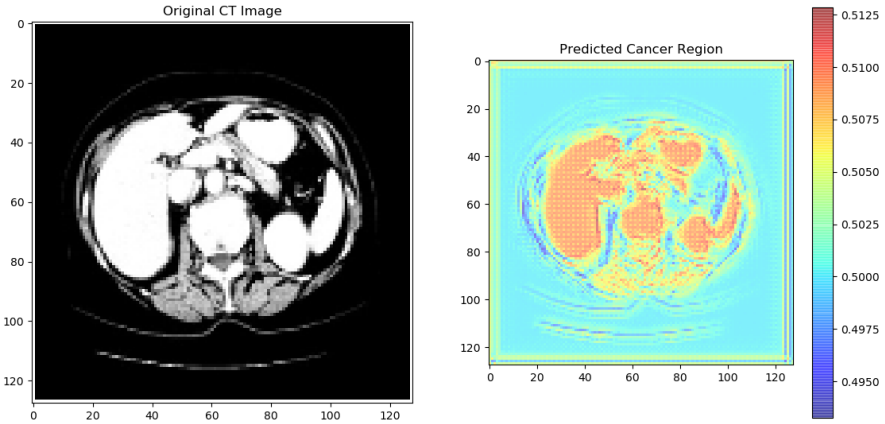

Figure 4. The original and predicted cancer region image

Table 2 shows the classification results by showing the comparison between various deep learning-based algorithm. The proposed EMCC obtains the high classification compare with other existing models as shown in Figure 5. These results are obtained based on the count values of the confusion matrix attributes. In this comparison, the lowest performance is shown by deep neural network-based Gabor features (DNN-GF) with the accuracy of 0.80%, Spc-0.99, Re-0.85, and F1S of 0.69%.

Table 2. The quantitative performance of liver cancer images using in terms of classification with EMCC

	ACC	Spc	Re	F1S
DNN-GF [24]	0.80	0.99	0.85	0.69
HI-DNN [25]	0.83	0.98	0.93	0.85
Coot optimization algorithm (COA) [4]	0.87	0.99	0.99	0.84
EMCC	0.97	0.99	0.99	0.97

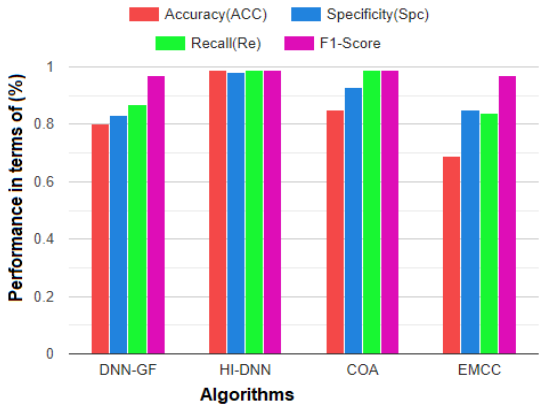

Figure 5. The comparison of liver cancer detection samples in terms of classification

7. CONCLUSION

This paper presented HepatoScan, an ensemble classification method for the detection and diagnosis of liver cancer tumors using liver cancer datasets. The proposed HepatoScan was an integrated method that categorizes the three types of liver cancer: hepatocellular carcinoma, cholangiocarcinoma, and angiosarcoma.

This paper demonstrated that the integrated method of EMCC exhibits superior efficacy in identifying lesions and classifying liver cancer tumors within the provided samples. The pre-trained model identifies precise and high-dimensional features through the convolutional layer in conjunction with the transfer learning layer. The pre-trained model demonstrates a minimal error loss in the loss function. The EMCC integrates U-Net and Mask R-CNN to identify abnormal (cancerous cells or tumors) and normal tissues. The encoder, bottleneck layer, and decoder execute the U-Net function. We employ the Mask R-CNN to detect the anomalous regions in the provided input image. The final layer combines the mask and bounding box to delineate precise regions. The classification outcomes demonstrate that the proposed method attains an accuracy of 0.97%, specificity of 0.99%, recall of 0.99%, and F1 score of 0.97%. All these values indicate a high degree of superior classification.

FUNDING INFORMATION

This research did not receive any specific grant from funding agencies in the public, commercial, or not-for-profit sectors.

AUTHOR CONTRIBUTIONS STATEMENT

This journal uses the Contributor Roles Taxonomy (CRediT) to recognize individual author contributions, reduce authorship disputes, and facilitate collaboration.

Name of Author	C	M	So	Va	Fo	I	R	D	O	E	Vi	Su	P	Fu
Tella Sumallika	✓	✓	✓	✓	✓	✓		✓	✓	✓			✓	
Raavi Satya Prasad		✓				✓		✓	✓	✓	✓	✓		

C : **C**onceptualization
M : **M**ethodology
So : **So**ftware
Va : **Va**lidation
Fo : **Fo**rmal analysis
I : **I**nvestigation
R : **R**esources
D : **D**ata Curation
O : Writing - **O**riginal Draft
E : Writing - Review & **E**diting
Vi : **Vi**sualization
Su : **Su**pervision
P : **P**roject administration
Fu : **Fu**nding acquisition

CONFLICT OF INTEREST STATEMENT

Authors state no conflict of interest.

DATA AVAILABILITY

No new data were generated or analyzed during this study. All data used are from publicly available sources cited in the manuscript.

REFERENCES

[1] A. Dutta and A. Dubey, "Detection of liver cancer using image processing techniques," in *2019 International Conference on Communication and Signal Processing (ICCSP)*, Apr. 2019, pp. 315–318, doi: 10.1109/ICCSP.2019.8698033.
[2] S. Charan, G. Uganya, and M. N. Kumar, "Comparison of accuracy and sensitivity in liver cancer segmentation of magnetic resonance images using convolutional neural network in comparison with support vector machine," in *2022 14th International Conference on Mathematics, Actuarial Science, Computer Science and Statistics (MACS)*, 2022, pp. 1–9, doi: 10.1109/MACS56771.2022.10023048.
[3] G. L. Kulkarni, S. S. Sannakki, and V. S. Rajpurohit, "Texture feature analysis for the liver cancer diseases using statistical based feature extraction technique," in *2020 Fourth International Conference on I-SMAC (IoT in Social, Mobile, Analytics and Cloud) (I-SMAC)*, 2020, pp. 1028–1033, doi: 10.1109/I-SMAC49090.2020.9243496.
[4] K. Sridhar, C. Kavitha, W. C. Lai, and B. P. Kavin, "Detection of liver tumour using deep learning based segmentation with coot extreme learning model," *Biomedicines*, vol. 11, no. 3, 2023, doi: 10.3390/biomedicines11030800.
[5] B. Lakshmipriya, B. Pottakkat, and G. Ramkumar, "Deep learning techniques in liver tumour diagnosis using CT and MR imaging-A systematic review," *Artificial Intelligence in Medicine*, vol. 141, 2023, doi: 10.1016/j.artmed.2023.102557.
[6] M. Chen *et al.*, "Classification and mutation prediction based on histopathology H&E images in liver cancer using deep learning," *npj Precision Oncology*, vol. 4, no. 1, 2020, doi: 10.1038/s41698-020-0120-3.
[7] K. Chaudhary, O. B. Poirion, L. Lu, and L. X. Garmire, "Deep learning–based multi-omics integration robustly predicts survival in liver cancer," *Clinical Cancer Research*, vol. 24, no. 6, pp. 1248–1259, 2018, doi: 10.1158/1078-0432.CCR-17-0853.
[8] J. Gregory, M. Dioguardi Burgio, G. Corrias, V. Vilgrain, and M. Ronot, "Evaluation of liver tumour response by imaging," *JHEP Reports*, vol. 2, no. 3, 2020, doi: 10.1016/j.jhepr.2020.100100.
[9] C. J. Wang *et al.*, "Deep learning for liver tumor diagnosis part II: convolutional neural network interpretation using radiologic imaging features," *European Radiology*, vol. 29, no. 7, pp. 3348–3357, 2019, doi: 10.1007/s00330-019-06214-8.
[10] V. Vekariya, T. Goswami, S. Singh, K. Ghodke, I. S. Abdulrahman, and A. Jain, "Determination of accuracy of neural network method using magnetic resonance images in finding liver cancer level," in *2023 3rd International Conference on Advance Computing and Innovative Technologies in Engineering (ICACITE)*, 2023, pp. 702–705, doi: 10.1109/ICACITE57410.2023.10182903.

[11] S. H. Zhen *et al.*, "Deep learning for accurate diagnosis of liver tumor based on magnetic resonance imaging and clinical data," *Frontiers in Oncology*, vol. 10, 2020, doi: 10.3389/fonc.2020.00680.
[12] O. I. Alirr, "Deep learning and level set approach for liver and tumor segmentation from CT scans," *Journal of Applied Clinical Medical Physics*, vol. 21, no. 10, pp. 200–209, 2020, doi: 10.1002/acm2.13003.
[13] T. Sumallika and R. S. Prasad, "A combined ensemble model (CEM) for a liver cancer detection system," *International Journal of Advanced Computer Science and Applications*, vol. 15, no. 2, pp. 163–172, 2024, doi: 10.14569/IJACSA.2024.0150218.
[14] T. Sumallika and R. S. Prasad, "LiverScope: an automated deep classification of liver cancer detection," *2025 6th International Conference on Mobile Computing and Sustainable Informatics (ICMCSI)*, Goathgaun, Nepal, 2025, pp. 1669-1673, doi: 10.1109/ICMCSI64620.2025.10883361.
[15] L. Liu *et al.*, "CT image segmentation method of liver tumor based on artificial intelligence enabled medical imaging," *Mathematical Problems in Engineering*, vol. 2021, 2021, doi: 10.1155/2021/9919507.
[16] S. Di, Y. Zhao, M. Liao, Z. Yang, and Y. Zeng, "Automatic liver tumor segmentation from CT images using hierarchical iterative superpixels and local statistical features," *Expert Systems with Applications*, vol. 203, 2022, doi: 10.1016/j.eswa.2022.117347.
[17] Y. Li, B. Zou, and Q. Liu, "A deep attention network via high-resolution representation for liver and liver tumor segmentation," *Biocybernetics and Biomedical Engineering*, vol. 41, no. 4, pp. 1518–1532, 2021, doi: 10.1016/j.bbe.2021.08.010.
[18] P. Gunasekhar and S. Vijayalakshmi, "Optimal biomarker selection using adaptive social ski-driver optimization for liver cancer detection," *Biocybernetics and Biomedical Engineering*, vol. 40, no. 4, pp. 1611–1625, 2020, doi: 10.1016/j.bbe.2020.10.005.
[19] A. Baâzaoui, W. Barhoumi, A. Ahmed, and E. Zagrouba, "Semi-automated segmentation of single and multiple tumors in liver CT images using entropy-based fuzzy region growing," *IRBM-Innovation and Research in BioMedical engineering*, vol. 38, no. 2, pp. 98–108, 2017, doi: 10.1016/j.irbm.2017.02.003.
[20] A. Das and S. K. Sabut, "Kernelized fuzzy c-means clustering with adaptive thresholding for segmenting liver tumors," *Procedia Computer Science*, vol. 92, pp. 389–395, 2016, doi: 10.1016/j.procs.2016.07.395.
[21] S. Kolli, B. R. Parvathala, and A. V. P. Krishna, "A novel liver tumor classification using improved probabilistic neural networks with Bayesian optimization," *e-Prime-Advances in Electrical Engineering, Electronics and Energy*, vol. 8, 2024, doi: 10.1016/j.prime.2024.100514.
[22] J. Kaur and P. Kaur, "PSO-PSP-Net + InceptionV3: An optimized hyper-parameter tuned computer-aided diagnostic model for liver tumor detection using CT scan slices," *Biomedical Signal Processing and Control*, vol. 95, 2024, doi: 10.1016/j.bspc.2024.106442.
[23] N. Khaled, H. Tarek, M. Makram, and A. Mohammed, "Enhanced diagnosis of liver cancer subtypes through deep learning techniques," in *2024 6th International Conference on Computing and Informatics (ICCI)*, 2024, pp. 189–194, doi: 10.1109/ICCI61671.2024.10485178.
[24] B. Ashreetha, M. R. Devi, U. P. Kumar, M. K. Mani, D. N. Sahu, and P. C. S. Reddy, "Soft optimization techniques for automatic liver cancer detection in abdominal liver images," *International Journal of Health Sciences*, vol. 6, pp. 10820–10831, 2022, doi: 10.53730/ijhs.v6ns1.7597.
[25] M. Rela, N. R. Suryakari, and R. R. Patil, "A diagnosis system by U-Net and deep neural network enabled with optimal feature selection for liver tumor detection using CT images," *Multimedia Tools and Applications*, vol. 82, no. 3, pp. 3185–3227, 2023, doi: 10.1007/s11042-022-13381-2.

BIOGRAPHIES OF AUTHORS

Tella Sumallika working as an assistant professor in Department of Information Technology in Gudlavalleru Engineering College, having 12 years of experience. She pursuing Ph.D. in computer science and engineering, Acharya Nagarjuna University. She received M.Tech. in computer science engineering from Pydah Engineering College in 2011. Current research interests include big data analytics, IoT, and machine learning. She published 8 research papers in various journals, presented 4 papers in various conferences, applied research works in DST, SERB. She received appreciation certificate for the best performance in teaching. She received Elite+Gold, elite online-course certificates for various subjects from NPTEL, sun certification in JAVA. She is working in a progressive and challenging environment, where she can enhance skills and potentials to the best and exploit them to create new avenues in the field of information technology. She can be contacted at email: sumallika.p@gmail.com.

Raavi Satya Prasad obtained his B.Sc. (1981) and M.Sc. with a Gold Medal (1983) from Nagarjuna University, followed by M.Phil. studies at the same institution. He later earned an M.Tech. in computer science (First Class) from Acharya Nagarjuna University in 2010 and a Ph.D. in half logistic software reliability growth model from the same university. Currently, he is a Professor and Dean in Dhanekula Institute of Engineering and Technology-JNTU Kakinada, Vijayawada. He can be contacted at email: deanresearch@diet.ac.in or profrsp@gmail.com.